

Electronic Supplementary Information

A Turn-On Fluorescent Probe based on Si-Rhodamine for Sensitive and
Selective Detection of Phosgene in Solutions and in the Gas Phase

Man Du, Baolong Huo, Jiemin Liu^{*}, Mengwen Li, Ao Shen, Xue Bai, Yaru
Lai, Leqiu Fang, Yunxu Yang^{*}

*Department of Chemistry and Chemical Engineering, School of Chemistry and
Biological Engineering, University of Science and Technology Beijing, Beijing
100083, China*

***Corresponding Author:** Yunxu Yang, Jiemin Liu

E-mail addresses: yxyang@ustb.edu.cn (Yunxu Yang);

liujm@ustb.edu.cn (Jiemin Liu)

Contents:

ESI1. Table S1 Comparisons of proposed method with recently reported strategies for phosgene detection.	3
ESI2. Fig. S1 Structures of probes recently reported for phosgene detection.	4
ESI3. Fig. S2 ¹ H NMR spectrum of compound DASE in CDCl ₃ -d ₁ .	5
ESI4. Fig. S3 ¹³ C NMR spectrum of compound DASE in CDCl ₃ -d ₁ .	5
ESI5. Fig. S4 HRMS spectrum of compound DASE in CH ₃ OH.	6
ESI6. Fig. S5 ¹ H NMR spectrum of compound SiR-carboxyl in CD ₃ OD-d ₄ .	6
ESI7. Fig. S6 ¹³ C NMR spectrum of compound SiR-carboxyl in CD ₃ OD-d ₄ .	7
ESI8. Fig. S7 HRMS spectrum of compound SiR-carboxyl in CH ₃ OH.	7
ESI9. Fig. S8 ¹ H NMR spectrum of compound SiR-amide in CD ₃ OD-d ₄ .	8
ESI10. Fig. S9 ¹³ C NMR spectrum of compound SiR-amide in CD ₃ OD-d ₄ .	8
ESI11. Fig.S10 HRMS spectrum of compound SiR-amide in CH ₃ OH.	9
ESI12. DFT Calculations.	10
ESI13. Detection limit	
Fig. S11 The linear relationship between the fluorescence intensity and phosgene concentration.	14
ESI14. Kinetic studies	
Fig. S12 <i>Pseudo</i> -first-order kinetic plot.	15
ESI15. Fig. S13 The reaction mechanism of SiR-amide with phosgene.	16
ESI16. Fig. S14 ESI-MS spectrum of SiR-amide upon addition of phosgene.	17
ESI17. References	18

ESI1.

Table S1. Comparisons of proposed method with recently reported strategies for phosgene detection.

Name/Literature	Mechanism	Fluorophore	Wavelength/nm	Detection limit	Dynamic range	Response time
dRB-EDA ^[1]	opening of the spiro-(deoxy)lactam	Rhodamine	$\lambda_{\text{ex}} = 560 \text{ nm}$, $\lambda_{\text{em}} = 590 \text{ nm}$	50 nM (phosgene)	—	—
Phos-1 ^[2]	ICT	4,5-diamino-1,8-naphthalimide	$\lambda_{\text{ex}} = 410 \text{ nm}$, $\lambda_{\text{em}} = 442 \text{ nm}$	1.3 nM (phosgene)	—	20 min
1-oxime ^[3]	Dehydration of oxime	BODIPY	$\lambda_{\text{ex}} = 530 \text{ nm}$, $\lambda_{\text{em}} = 570 \text{ nm}$	0.09 ppb (phosgene)	—	10 s
IC-phos ^[4]	ICT	3-benzimidazole iminocoumarin	$\lambda_{\text{ab}} = 425 \text{ nm}$, $\lambda_{\text{em}} = 482 \text{ nm}$	27 nM (phosgene)	0 to 7.5 μM	2 min
OPD-TPE-Py-2CN ^[5]	AIE	tetraphenylethene	$\lambda_{\text{ex}} = 365 \text{ nm}$, $\lambda_{\text{em}} = 475 \text{ nm}$	1.87 ppm (phosgene)	0 to 15 ppm	2 min
Probe 1 ^[6]	ESIPT	2-(2-aminophenyl) benzothiazole	$\lambda_{\text{ex}} = 475 \text{ nm}$, $\lambda_{\text{em}} = 545 \text{ nm}$	0.14 ppm (phosgene)	0-3.0 μM	—
Sensor 1 ^[7]	spirocyclic ring-open reaction	benzimidazole-fused rhodamine	$\lambda_{\text{ex}} = 530 \text{ nm}$, $\lambda_{\text{em}} = 578 \text{ nm}$	3.2 ppb (phosgene)	—	2 min
Sensor 2 ^[8]	Intramolecular cyclization	7-hydroxycoumarin	$\lambda_{\text{ex}} = 375 \text{ nm}$, $\lambda_{\text{em1}} = 445 \text{ nm}$, $\lambda_{\text{em2}} = 495 \text{ nm}$	1 nM (phosgene)	—	—
NBD-OPD ^[9]	Reaction between OPD and phosgene	4-chloro-7-nitrobenzo [c][1,2,5]oxadiazole	$\lambda_{\text{ex}} = 270 \text{ nm}$, $\lambda_{\text{em}} = 315 \text{ nm}$	7 nM (phosgene)	—	2 min
RB-OPD ^[9]	Reaction between OPD and phosgene	Rhodamine	$\lambda_{\text{ex}} = 530 \text{ nm}$, $\lambda_{\text{em}} = 575 \text{ nm}$	28 nM (phosgene)	—	1 min
NAP-OPD ^[9]	Reaction between OPD and phosgene	1,8-naphthalimide	$\lambda_{\text{ex}} = 340 \text{ nm}$, $\lambda_{\text{em}} = 480 \text{ nm}$	28 nM (phosgene)	—	3 min
Phos-2 ^[10]	ESIPT	peridiamine of naphthalimide	$\lambda_{\text{ex}} = 400 \text{ nm}$, $\lambda_{\text{em}} = 468 \text{ nm}$	0.2 nM (triphosgene)	—	6 min
o-Pab ^[11]	PET	BODIPY	$\lambda_{\text{ex}} = 450 \text{ nm}$, $\lambda_{\text{em}} = 530 \text{ nm}$	2.7 nM (phosgene)	—	15 s
8-EDAB ^[12]	ICT	BODIPY	$\lambda_{\text{ex}} = 465 \text{ nm}$, $\lambda_{\text{em}} = 512 \text{ nm}$	0.12 nM (phosgene)	0-3.5 μM	15 s
BTA ^[13]	ICT	benzothiadiazole	$\lambda_{\text{ex}} = 380 \text{ nm}$, $\lambda_{\text{em}} = 508 \text{ nm}$	20 nM (phosgene)	—	20 min
o-Pac ^[14]	PET	BODIPY	$\lambda_{\text{ex}} = 368 \text{ nm}$, $\lambda_{\text{em}} = 446 \text{ nm}$	3 nM (phosgene)	0-50 μM	0.5 min
This work	conversion of amide to nitrile	Si-rhodamine	$\lambda_{\text{ex}} = 653 \text{ nm}$, $\lambda_{\text{em}} = 679 \text{ nm}$	8.9 nM (triphosgene)	0.5-10 μM	4 min

“—“ Not mentioned.

ESI2.

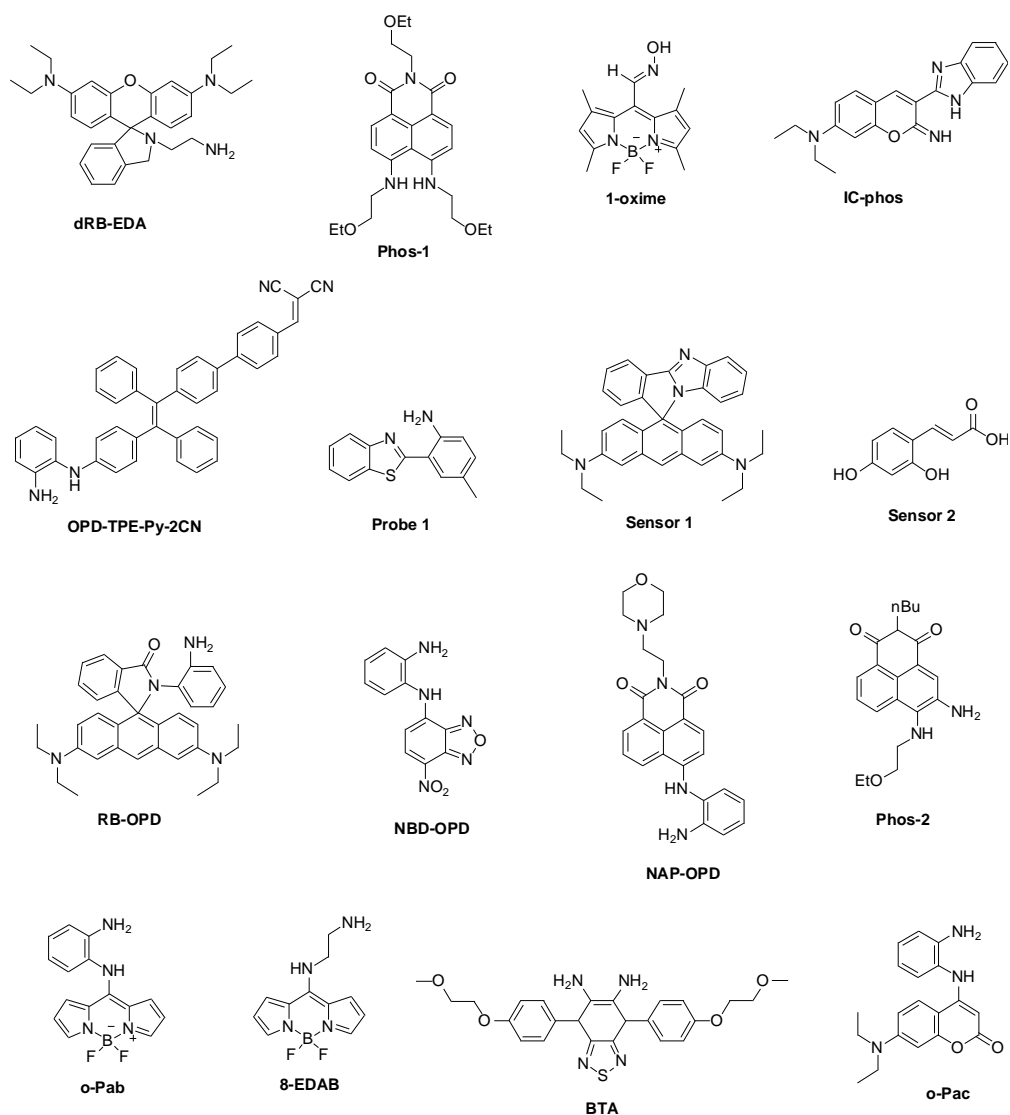


Fig. S1. Structures of probes recently reported for phosgene detection.

ESI3.

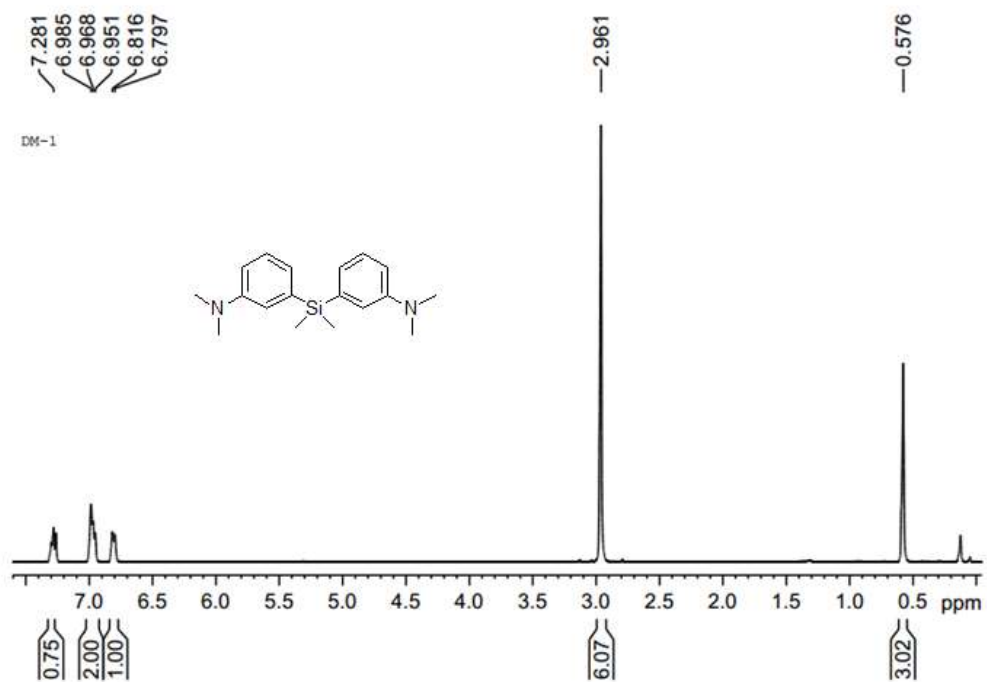


Fig. S2. ¹H NMR spectrum of compound **DASE** in CDCl₃-d₁.

ESI4.

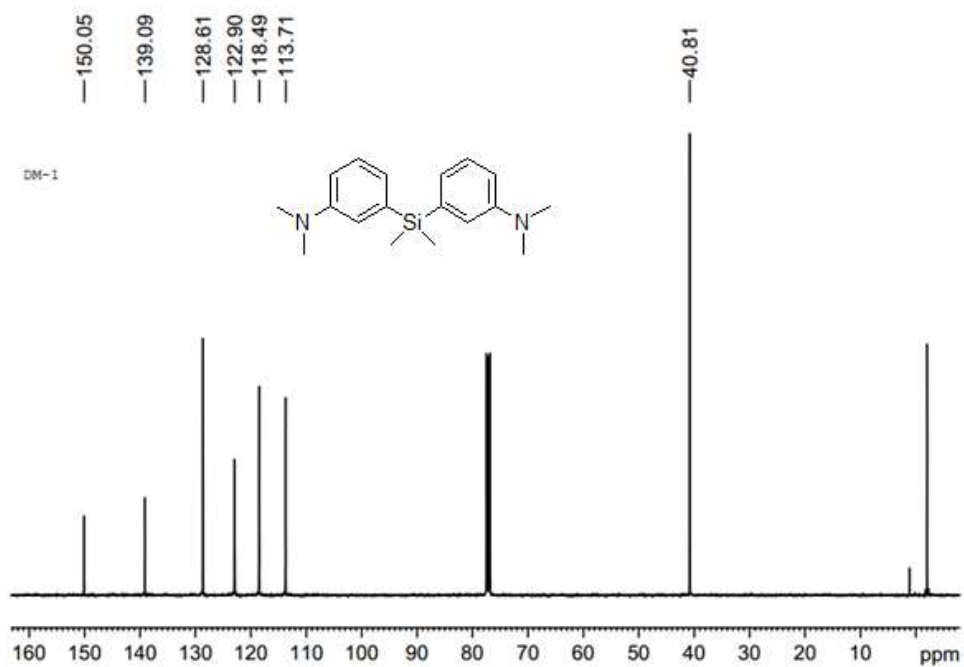


Fig. S3. ¹³C NMR spectrum of compound **DASE** in CDCl₃-d₁.

ESI5.

Dama-106 #11 RT: 0.11 AV: 1 NL: 425E9
T: FIMS +pESI Full ms [50.00-750.00]

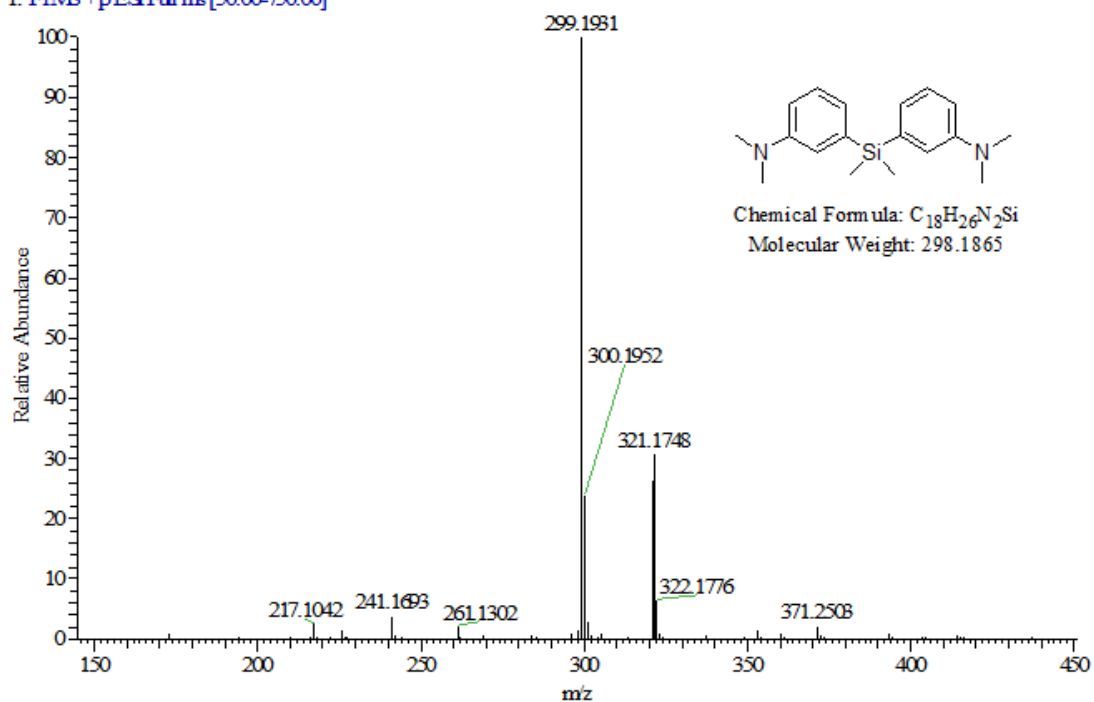


Fig. S4. HRMS spectrum of compound DASE in CH_3OH .

ESI6.

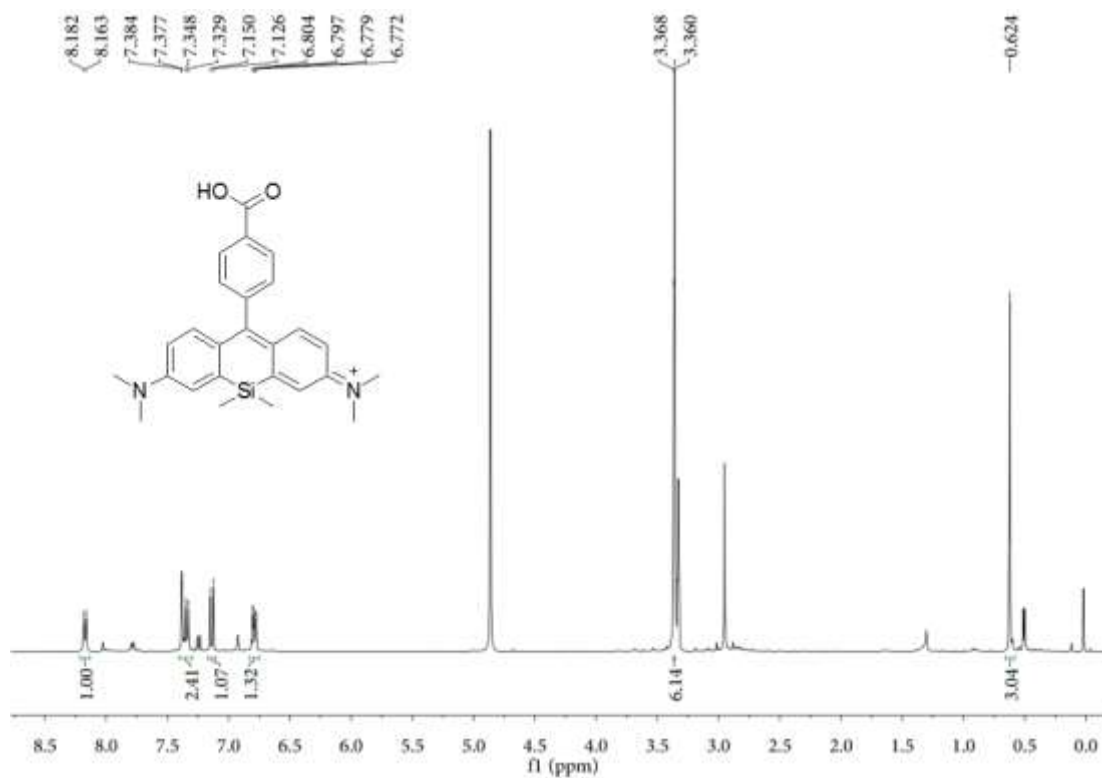


Fig. S5. 1H NMR spectrum of compound SiR-carboxyl in CD_3OD-d_4 .

ESI7.

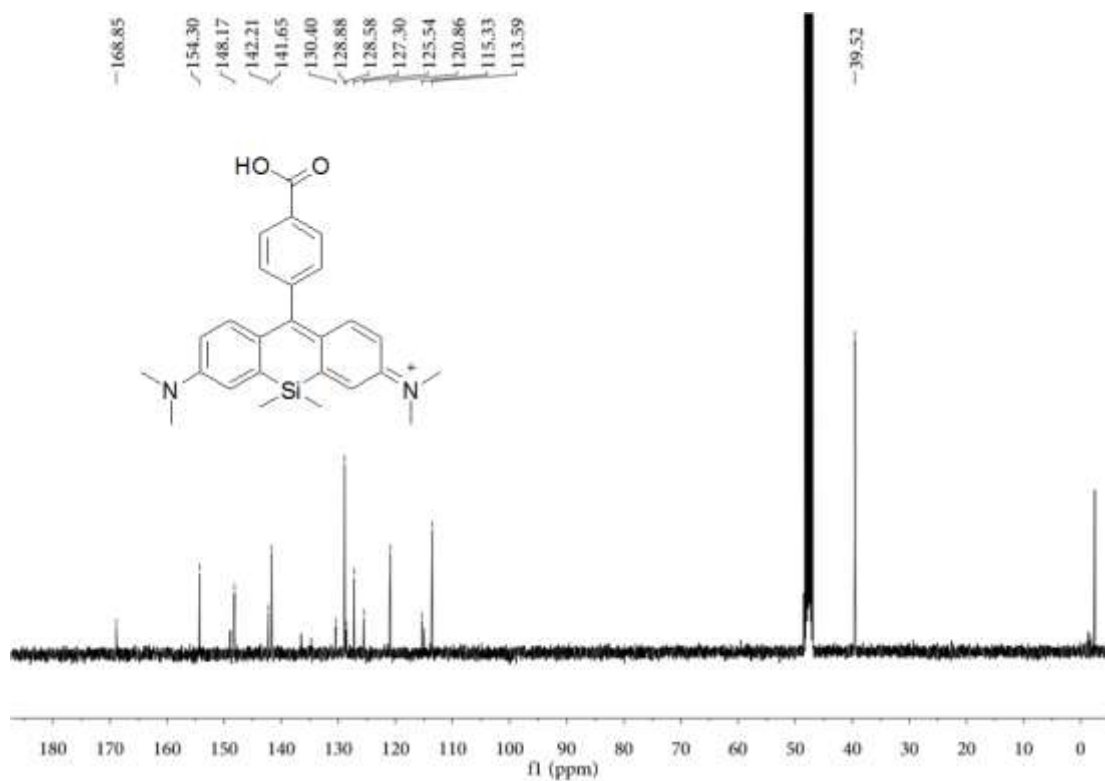


Fig. S6. ^{13}C NMR spectrum of compound SiR-carboxyl in $\text{CD}_3\text{OD}-d_4$.

ESI8.

2018011703 #11 RT: 0.10 AV: 1 NL: 5.08ES
T: FIMS+p ESI Full ms [50.0000-750.0000]

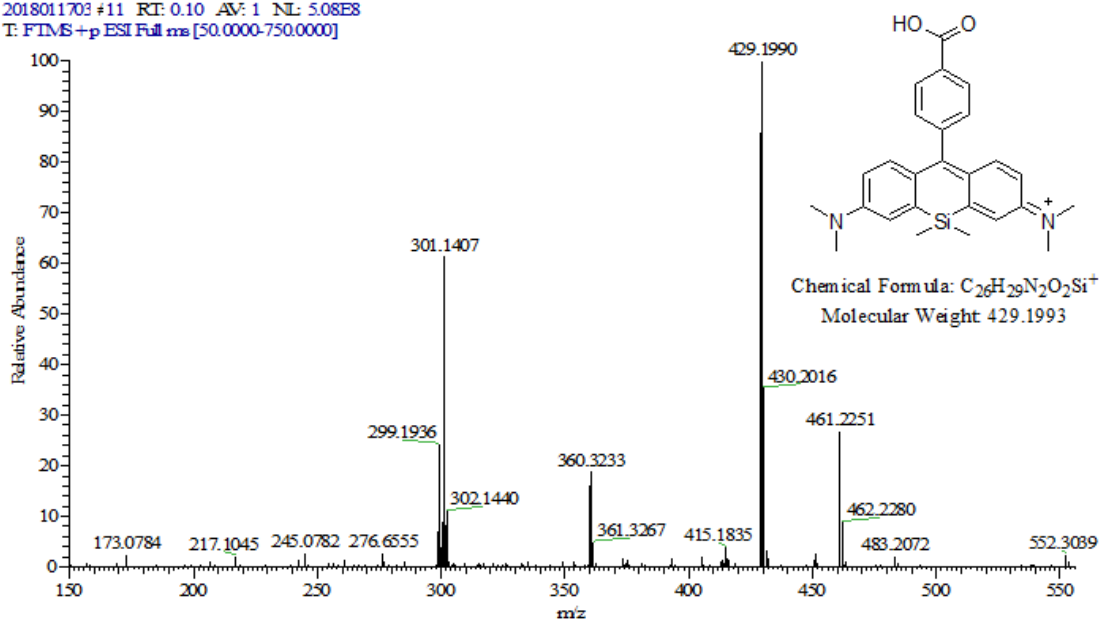
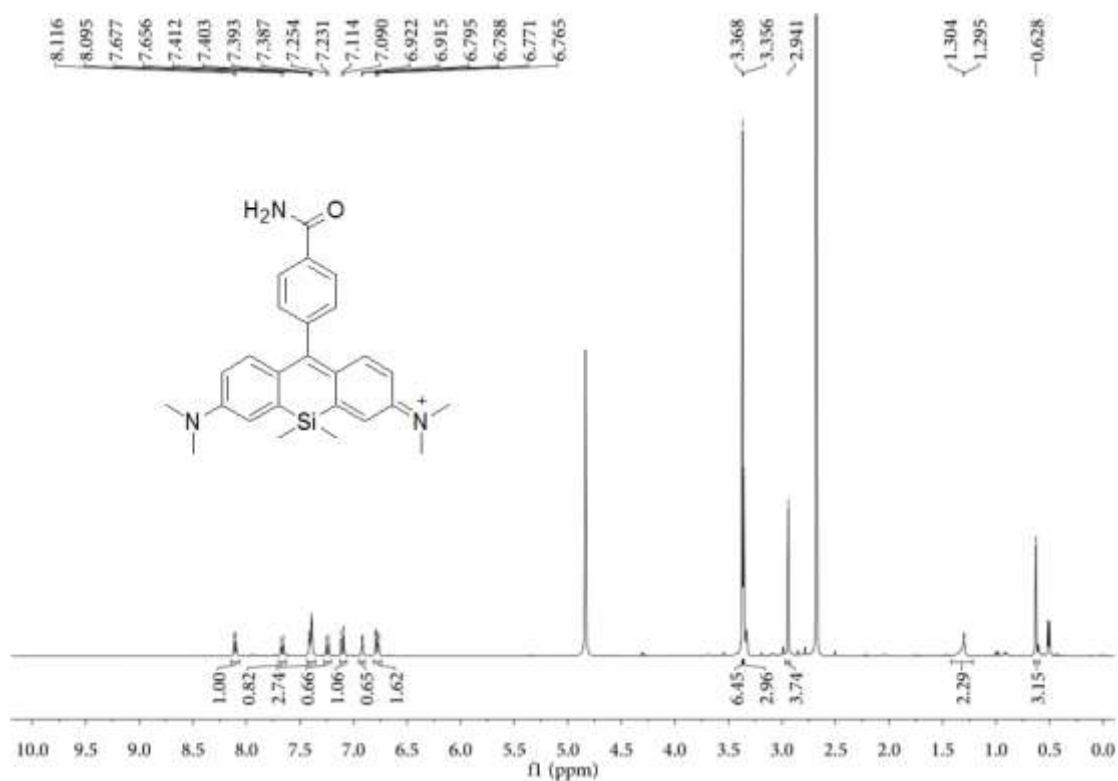
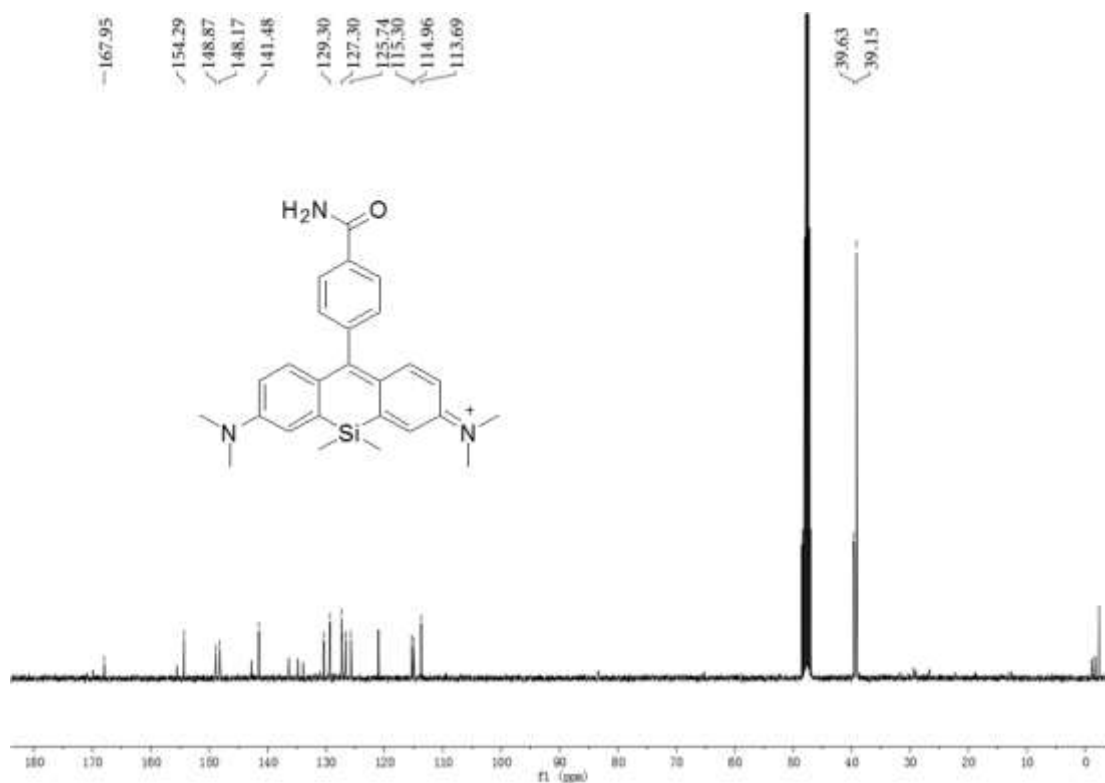


Fig. S7. HRMS spectrum of probe compound SiR-carboxyl in CH_3OH .

ESI9.**Fig. S8.** ¹H NMR spectrum of compound SiR-amide in CD₃OD-d₄.**ESI10.****Fig. S9.** ¹³C NMR spectrum of compound in SiR-amide CD₃OD-d₄.

ESI11.

2018011702 #11 RT: 0.10 AV: 1 NL: 2.07ES
T: FTMS+p ESI Full ms [50.0000-750.0000]

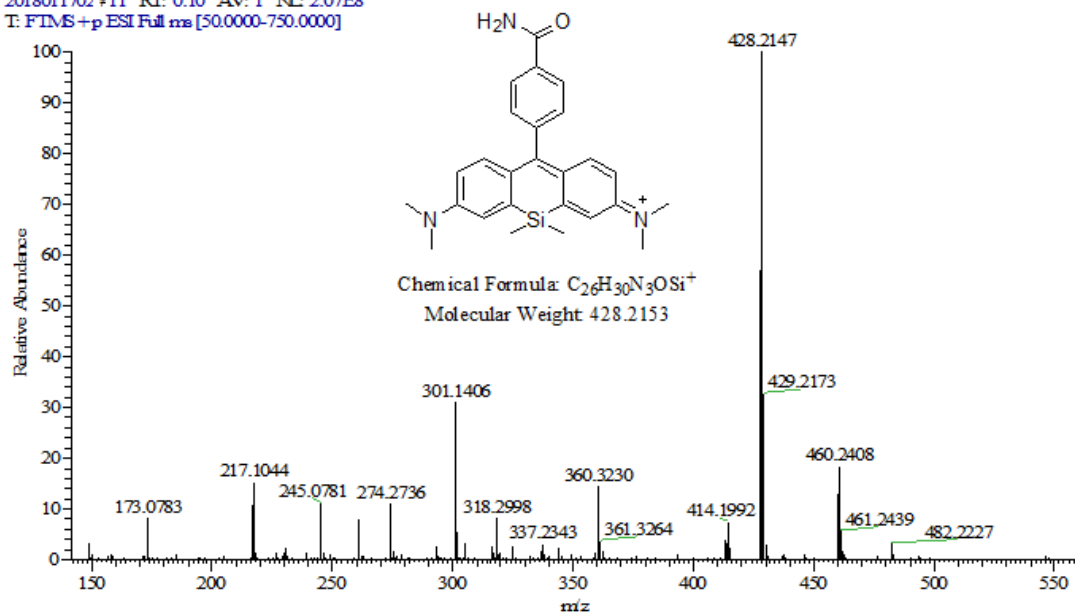


Fig. S10. HRMS spectrum of probe compound **SiR-amide** in CH_3OH .

ESI12

DFT Calculations

Geometric optimizations and energy level calculations were performed in the gas phase at the B3LYP 6-311++G (d, p) level of theory, using the Gaussian 09 software package. Absolute energies in Hartrees are given without additional corrections.

• Cartesian Coordinates for **SiR-amide** (Energy : -1537.6620747 hartrees):

C	0.541054	-3.679247	-0.014228
C	0.881765	-2.350283	-0.010420
C	-0.088259	-1.298849	0.007858
C	-1.471589	-1.697691	0.018418
C	-1.803835	-3.038031	0.015617
C	-0.825535	-4.080667	0.000348
C	-1.908432	1.213029	0.006646
C	-0.469101	1.235599	0.006355
C	0.151049	2.523957	0.002277
H	1.231700	2.590104	0.006705
C	-0.563087	3.695618	-0.009563
C	-1.987277	3.680575	-0.017253
C	-2.618156	2.397862	-0.004766
H	1.330426	-4.419869	-0.031193
H	1.934745	-2.099289	-0.025663
H	-2.852039	-3.316601	0.023129
H	-0.024496	4.634683	-0.013962
H	-3.702030	2.357410	-0.004559
C	3.936972	0.525037	1.200116
C	4.628891	0.663631	-0.009338
C	3.913965	0.599323	-1.211876
C	2.533991	0.419588	-1.208503
C	2.554583	0.335471	1.208071
H	4.472170	0.525607	2.145288
H	4.465068	0.684293	-2.142585
H	1.991066	0.374715	-2.148615
H	2.031253	0.215790	2.152713
C	6.123748	0.836121	-0.108720
O	6.718860	0.589509	-1.148286
N	6.769993	1.244032	1.029845
H	7.754441	1.452755	0.922028
H	6.280775	1.747421	1.755444
C	1.839809	0.283749	0.003738
C	0.352592	0.062931	0.008485
N	-1.181774	-5.388282	-0.002599
C	-2.591958	-5.780897	0.008622
H	-3.116451	-5.406133	-0.878057
H	-2.658010	-6.868107	0.008033

H	-3.101028	-5.408310	0.905033
C	-0.157914	-6.435415	-0.024163
H	0.490108	-6.373838	0.857564
H	-0.644943	-7.409665	-0.021750
H	0.462826	-6.364358	-0.924673
Si	-2.850559	-0.416587	0.029941
C	-3.928084	-0.587255	-1.509910
H	-4.704554	0.186353	-1.536022
H	-3.334556	-0.498719	-2.425999
H	-4.435401	-1.559002	-1.530673
C	-3.883640	-0.564474	1.602616
H	-4.389570	-1.535933	1.651843
H	-3.264514	-0.462487	2.500202
H	-4.659067	0.209756	1.638992
N	-2.709629	4.827651	-0.034663
C	-2.035078	6.127453	-0.047034
H	-2.784717	6.917517	-0.064506
H	-1.416365	6.261530	0.847745
H	-1.401242	6.236353	-0.934531
C	-4.172927	4.792467	-0.042866
H	-4.564470	4.299846	0.854789
H	-4.552526	5.813212	-0.062642
H	-4.553049	4.269680	-0.928182

• Cartesian Coordinates for **SiR-nitrile** (Energy : -1461.1983057 hartrees):

C	3.728996	0.292265	-0.026698
C	2.465385	0.825848	-0.014101
C	1.281723	0.022326	0.001002
C	1.471482	-1.405084	0.008618
C	2.747636	-1.931962	-0.004814
C	3.924102	-1.119066	-0.024786
C	-1.471643	-1.404900	0.008442
C	-1.281753	0.022487	0.000917
C	-2.465342	0.826122	-0.014021
H	-2.374752	1.905091	-0.017392
C	-3.728994	0.292636	-0.026586
C	-3.924228	-1.118677	-0.024746
C	-2.747838	-1.931686	-0.004891
H	4.578201	0.963334	-0.038839
H	2.374836	1.904816	-0.017597
H	2.867007	-3.009815	0.000606
H	-4.578146	0.963774	-0.038640
H	-2.867300	-3.009532	0.000559
C	0.000755	4.261119	1.224653
C	0.000304	4.969005	0.011791
C	-0.000239	4.267021	-1.204542
C	-0.000342	2.874824	-1.203541
C	0.000679	2.868967	1.216829
H	0.001176	4.803958	2.164136
H	-0.000578	4.814489	-2.141334
H	-0.000768	2.337313	-2.147338
H	0.001053	2.326953	2.158042
C	0.000117	2.162535	0.004936
C	0.000024	0.658317	0.003508
N	5.163912	-1.664594	-0.040346
C	5.343665	-3.117635	-0.037968
H	4.880154	-3.576651	-0.918784
H	6.408902	-3.343879	-0.058704
H	4.915926	-3.569920	0.864313
C	6.351874	-0.807172	-0.057390
H	6.392352	-0.169082	0.832785
H	7.242774	-1.433673	-0.068945
H	6.367926	-0.171037	-0.949708
Si	-0.000150	-2.579507	0.052815
C	0.000069	-3.709812	-1.457829
H	-0.883696	-4.358734	-1.466319
H	0.002565	-3.133837	-2.389295
H	0.881457	-4.361992	-1.463580

C	-0.000530	-3.576972	1.654901
H	0.881606	-4.225168	1.716385
H	0.001725	-2.922927	2.533368
H	-0.885148	-4.221589	1.718232
N	-5.164094	-1.664084	-0.040221
C	-6.351976	-0.806542	-0.057058
H	-7.242945	-1.432958	-0.067876
H	-6.391933	-0.168097	0.832877
H	-6.368410	-0.170760	-0.949627
C	-5.343990	-3.117104	-0.038240
H	-4.916174	-3.569694	0.863852
H	-6.409253	-3.343239	-0.058883
H	-4.880645	-3.575914	-0.919253
C	0.000404	6.403291	0.015372
N	0.000485	7.565959	0.018422

ESI13.

Detection limit

The detection limit for phosgene was calculated by the fluorescence titration experiments according to the reported method. A good linear relationship between the fluorescence intensity and F^- concentration ($0.5 \mu\text{M}$ - $10 \mu\text{M}$) could be obtained ($R^2=0.9991$). The value obtained for the F^- was found to be 8.9 nM by the equation of $L_{OD}=3\delta/m$ (δ was the standard deviation of the blank solution and m is the absolute value of the slope between intensity versus F^- concentration). $\delta= 0.2772$, $m= 93.8384$.

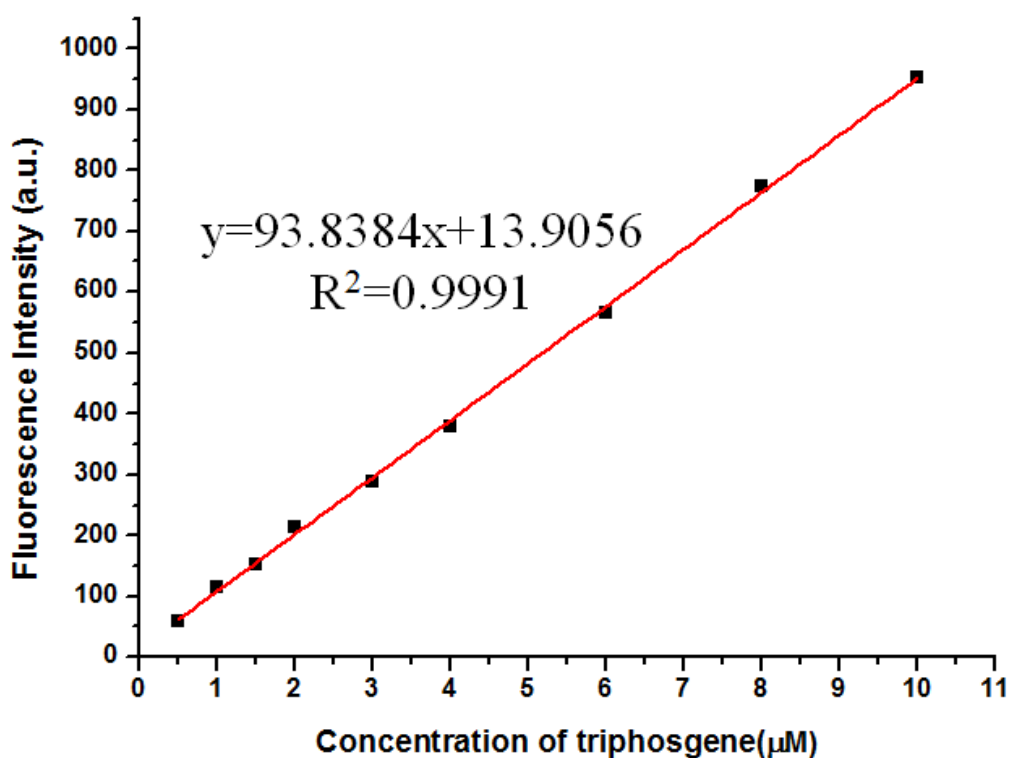


Fig. S11. The linear relationship between the fluorescence intensity and phosgene concentration (0.5 - $10 \mu\text{M}$) in CH_3CN . Excitation and emission were at $653 \text{ nm}/679 \text{ nm}$ respectively.

ESI14.

Kinetic studies:

The reaction of **SiR-amide** (10 μM) with phosgene in DMSO (pH 8.0, 30 % Tris-HCl) was monitored using the fluorescence intensity at 679 nm. The reaction was carried out at 25 $^{\circ}\text{C}$. The *pseudo*-first-order rate constant for the reaction was determined by fitting the fluorescence intensities of the samples to the *pseudo*-first-order equation:

$$\text{Ln} [(F_t - F_{\text{min}}) / F_{\text{min}}] = -k't$$

Where F_t and F_{min} are the fluorescence intensities at 679 nm at time t and the minimum value obtained after the reaction was complete. k' is the *pseudo*-first-order rate constant. The *pseudo*-first-order plots for the reaction of **SiR-amide** with 2 equiv. of phosgene is shown in Fig. S12, the *pseudo*-first-order rate constant $k' = 1/t_1 = 0.3966 \text{ min}^{-1}$.

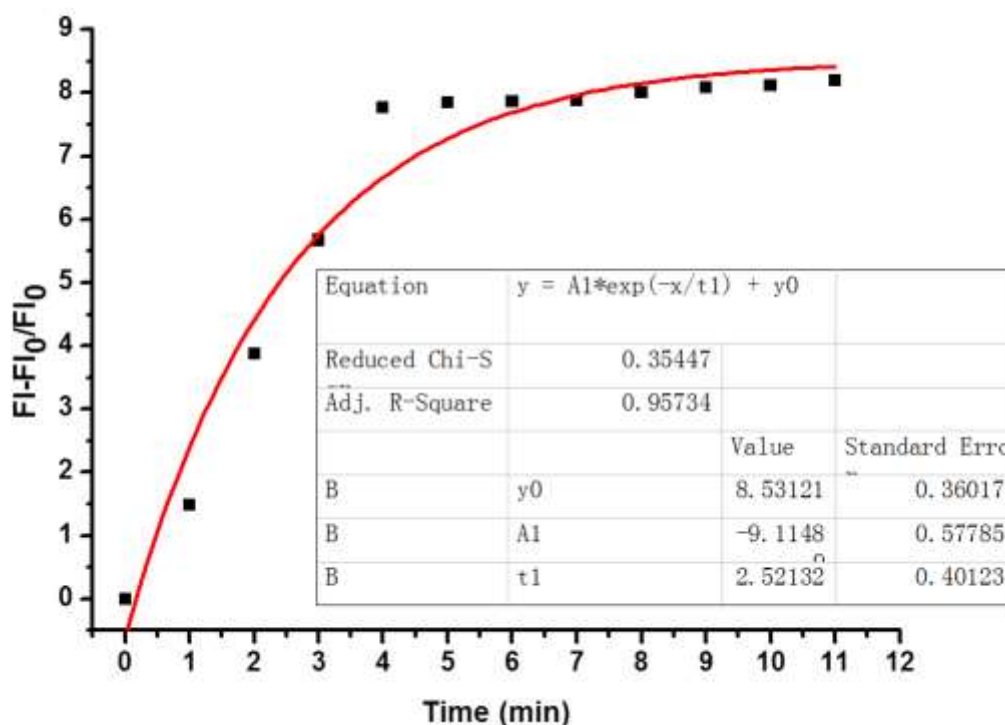


Fig. S12. *Pseudo*-first-order kinetic plot of the reaction of **SiR-amide** (10 μM) with phosgene (2 equiv.) in CH_3CN . $k = 0.3966 \text{ min}^{-1}$.

ESI15.

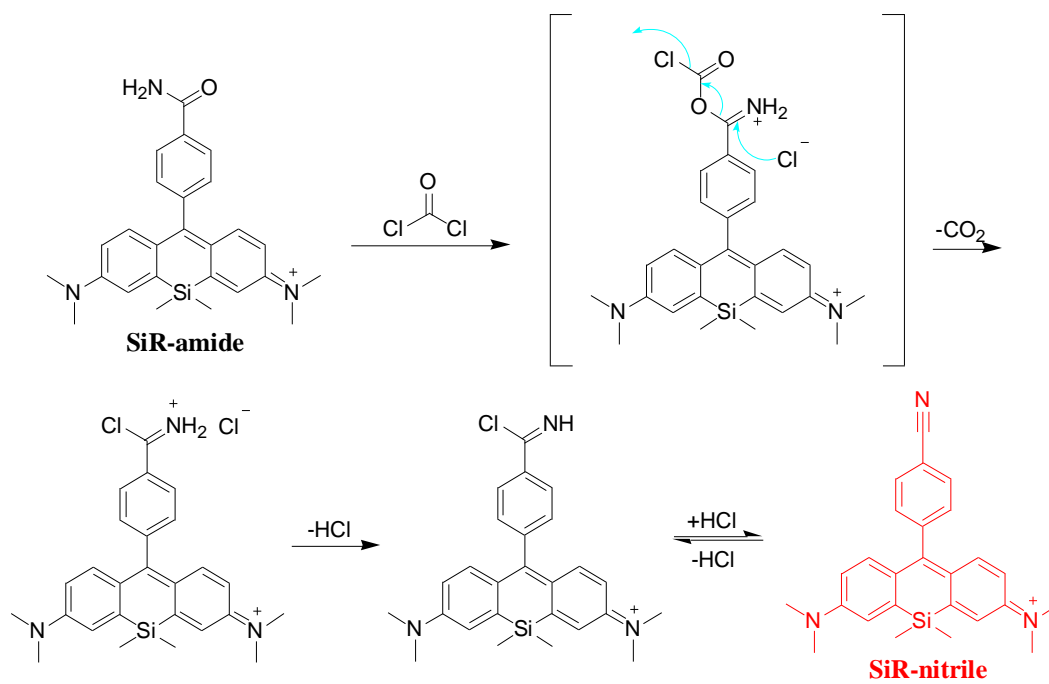


Fig. S13. The reaction mechanism of SiR-amide with phosgene.

ESI16.

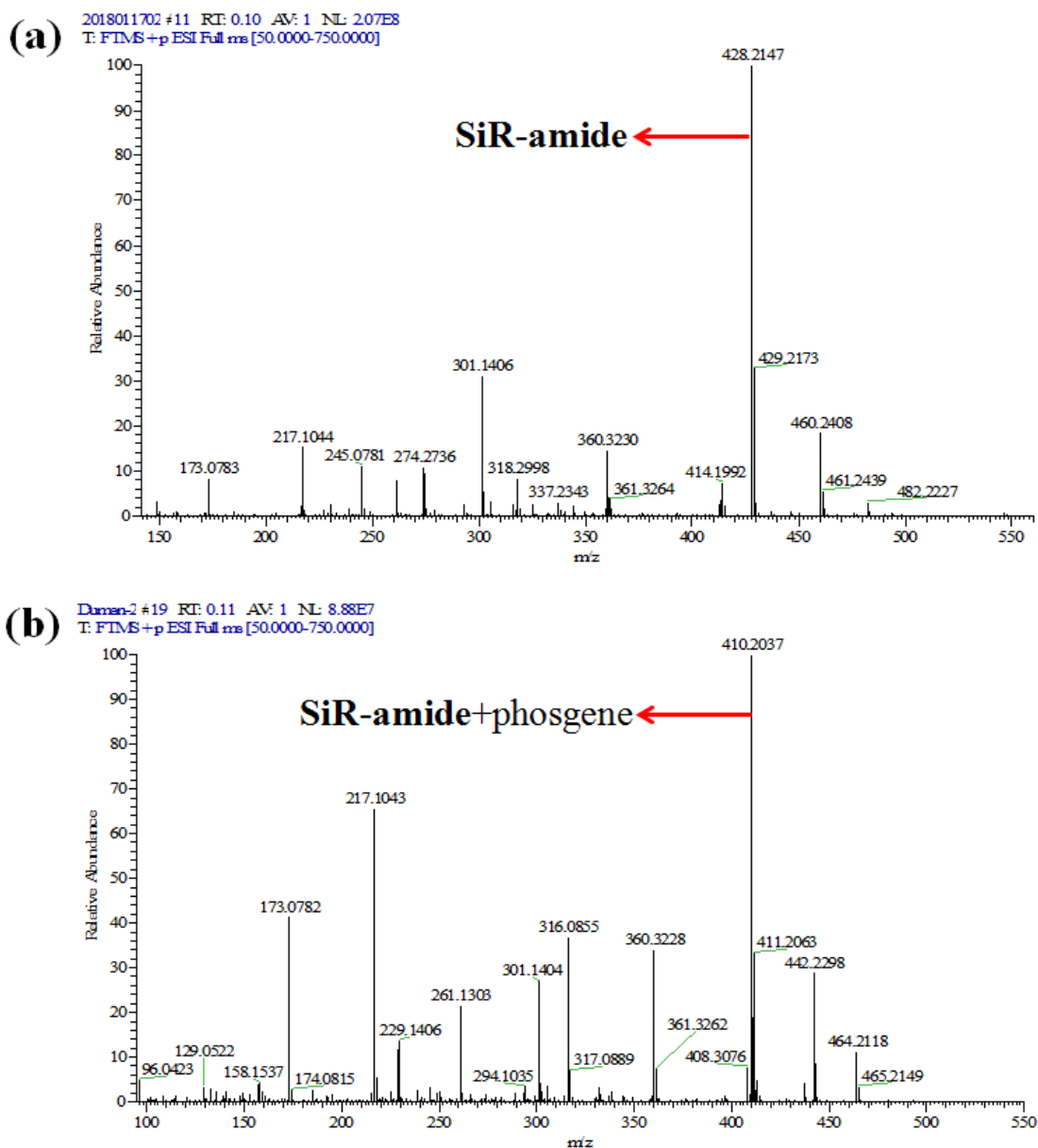


Fig. S14. ESI-MS spectrum (positive ion mode) of **SiR-amide** upon addition of phosgene in CH_3CN . (a) only **SiR-amide**, (b) the isolated aggregates of compound after **SiR-amide** reacted with phosgene for 5 min.

ESI17.

References

- [1] X. J. Wu, Z. S. Wu, Y. H. Yang and S. F. Han, *Chem. Commun.*, 2012, **48**, 1895.
- [2] S. L. Wang, L. Zhong, Q. H. Song and W. H. Zhu, *Chem. Commun.*, 2017, **53**, 1530.
- [3] T. I. Kim, B. Hwang, J. Bouffard and Y. Kim, *Anal. Chem.*, 2017, **89**, 12837.
- [4] W. Y. Feng, S. Y. Gong, E. B. Zhou, X. Y. Yin and G. Q. Feng, *Anal. Chim. Acta*, 2018, 1.
- [5] H. T. Xie, Y. L. Wu, F. Zeng, J. J. Chen and S. Z. Wu, *Chem. Commun.*, 2017, **53**, 9813.
- [6] L. Y. Chen, D. Wu, J. M. Kim and J. Yoon, *Anal. Chem.*, 2017, **89**, 12596.
- [7] Y. Hu, X. Zhou, H. Jung, S. J. Nam, M. H. Kim and J. Yoon, *Anal. Chem.*, 2018, **90**, 3382.
- [8] P. Kundu and K. C. Hwang, *Anal. Chem.*, 2012, **84**, 4594.
- [9] Y. Hu, L. Y. Chen, H. Jung, Y. Y. Zeng, S. Lee, K. M. K. Swamy, X. Zhou, M. H. Kim and J. Yoon, *ACS Appl. Mater. Interfaces*, 2016, **8**, 22246.
- [10] S. L. Wang, L. Zhong and Q. H. Song, *Chem. Eur. J.*, 2018, **24**, 5652.
- [11] H. C. Xia, X. H. Xu and Q. H. Song, *Anal. Chem.*, 2017, **89**, 4192.
- [12] Y. L. Zhang, A. D. Peng, X. K. Jie, Y. L. Lv, X. F. Wang and Z. Y. Tian, *ACS Appl. Mater. Interfaces*, 2017, **9**, 13920.
- [13] W. Q. Zhang, K. Cheng, X. Y. Yang, Q. Y. Li, H. Zhang, Z. Ma, H. Lu, H. Wu and X. J. Wang, *Org. Chem. Front.*, 2017, **4**, 1719.
- [14] H. C. Xia, X. H. Xu and Q. H. Song, *ACS Sens.*, 2017, **2**, 178.